Delta Baryon Photoproduction with Twisted Photons

Andrei Afanasev* and Carl E. Carlson

A future gamma factory at CERN or accelerator-based gamma sources elsewhere can include the possibility of energetic twisted photons, which are photons with a structured wave front that can allow a pre-defined large angular momentum along the beam direction. Twisted photons are potentially a new tool in hadronic physics, and one possibility is considered here, namely the photoproduction of Δ(1232) baryons using twisted photons. It is shown that particular polarization amplitudes isolate the smaller partial wave amplitudes and they are measurable without interference from the terms that are otherwise dominant.

1. Introduction

Twisted photons are examples of light with a structured wave front that can produce transitions with quantum number changes that are impossible with plane wave photons. One can envision a number of applications in the field of hadron structure that would require sources of twisted photons with MeV-GeV energy scales. Such energies are achievable via Compton up-conversion in high-energy electron collisions with twisted optical photons [1,2] or in twisted-photon collisions with high-energy ions, as recently suggested for CERN Gamma Factory.[3] Presently, HIGS facility is making important steps toward twisted-photon generation, [4] opening new opportunities for nuclear physics studies.

Herein, we will focus on how twisted light may contribute to measuring small but important contributions to the electromagnetic production of Δ(1232) baryons from nucleon targets.

More specifically, twisted photons are states with total angular momentum whose projection along the direction of motion can be any integer, m_γ, times $\hbar$. The Poynting vector or momentum density of these states swirls about a vortex line, and the intensity of the wavefront is typically zero or very small on the vortex line. (Indeed, the "hole" in the middle of the wavefront can find applications seemingly unconnected to the swirling of the states, as in stimulated emission spectroscopy studies; see ref. [5])

A. Afanasev
Department of Physics
The George Washington University
Washington, DC 20052, USA
E-mail: afanas@email.gwu.edu

C. E. Carlson
Physics Department
William & Mary
Williamsburg, VA 23187, USA

The ORCID identification number(s) for the author(s) of this article can be found under https://doi.org/10.1002/andp.202100228
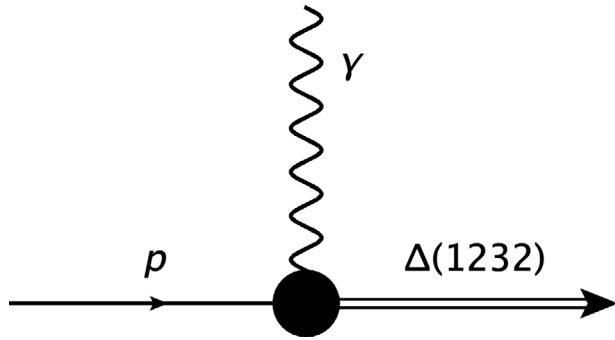
In photoabsorption, the photon's projected angular momentum m_γ is transferred to the target system and may be shared between internal excitation of the final state and orbital angular momentum of the final state's overall center-of-mass. That the final internal angular momentum projection can differ by m_γ units from that of the target allows transitions quite different from the plane wave case, where the photon necessarily transfers $m_\gamma = \Lambda = \pm 1$ to the final excitation. Here Λ is the helicity or spin along the direction of motion of the photon and that $\Lambda = \pm 1$ only is a standard fact for plane waves.

That large projected angular momentum transfer works in practice for atoms has been shown experimentally and reported in ref. [6], where optical orbital angular momentum was transferred to bound electrons, exciting $S_{1/2}$ to $D_{5/2}$ transitions in ^{40}Ca ions with quantum number changes beyond what a plane wave photon could induce. Further, the sharing of final state angular momentum between internal and overall degrees of freedom, when the ion was offset from the vortex line, was also measured and matched well with theoretical studies.[7,8]

The Δ(1232) is a spin 3/2 baryon that can be photoexcited from the nucleon (**Figure 1**) via $M1$ (with related notations M_{1+} and G_M^*) and $E2$ (ditto with E_{1+} or G_E^*) transitions. For a thorough review of electromagnetic excitation of the Δ(1232), see ref. [9]. In simple models, the Δ is dominantly a spatial S-state with a spin-3/2 spin wave function. This can be obtained from the nucleon by a simple spin flip, which an $M1$ transition can do, and there is a large N to Δ $M1$ amplitude. The $E2$ transition requires two units of orbital angular momentum, and must involve the small D-wave spatial component of the Δ or of the nucleon. Accurate knowledge of the $E2$ size would help elucidate the Δ composition and hadron structure generally.

Currently the particle data group [10] quotes an G_E^*/G_M^* ratio in the 2–3% range, based on plane wave photon cross section measurements where the $E2$ is neither the only nor the dominant contribution. We shall show that twisted photons can in principle produce signals there the $E2$ is the only contributor.

In much of what follows, it is more natural to describe plane wave Δ photoproduction using helicity amplitudes $\mathcal{M}_{m_i\Lambda}^{(pw)}$, where Λ is the helicity of the photon and m_i is the spin of the nucleon target along the photon's momentum direction. There are two independent helicity amplitudes

$$\mathcal{M}_{1/2,1}^{(pw)} \propto \sqrt{3}\left(G_M^* + G_E^*\right)$$

$$\mathcal{M}_{-1/2,1}^{(pw)} \propto G_M^* - 3G_E^* \tag{1}$$

2100228 (1 of 9)

**ADVANCED
SCIENCE NEWS**

www.advancedsciencenews.com

annalen
der **physik**

www.ann-phys.org

Figure 1. Photoexcitation of Δ(1232) baryon on a proton target.

and others can be obtained by parity transformation

$$\mathcal{M}^{(\text{pw})}_{-m_i,-\Lambda} = -\mathcal{M}^{(\text{pw})}_{m_i\Lambda} \tag{2}$$

In this notation, our goal is to use twisted photons to isolate physically achievable situations where the helicity amplitudes combine with the $M1$ contributions canceling and the $E2$ not.

The calculation of the N to Δ transition with twisted photons is in many ways analogous to atomic calculations. However, the most straightforward atomic calculations are made in a no-recoil limit, which gives accurate results for targets that are quite massive compared to the photon energy. For the the N to Δ transitions, we do take account of the recoil, eventually finding that the recoil corrections are small, at the level of a few percentage. Also, for the apparently simplest atomic analog, an $S_{1/2}$ to $D_{3/2}$ transition in a single electron atom, the $M1$ does not contribute at all to leading order. However, our crucial results are based on the properties of the twisted photon and on the quantum numbers and rotation properties of the hadronic states. A more exactly analogous atomic analog can be found among multi-electron atoms. In particular, there is an Boron-like example where the calculated $M1$ and $E2$ amplitudes are about the same size,[11] and we have elsewhere shown how twisted photons could be instrumental in measuring these amplitudes.[12]

In the following, Section 2 will contain some background material on twisted photons, which may be skipped or skimmed by readers already expert. Section 3 will, for the sake of beginning simply, find results for twisted photon induced N to Δ transitions in the no-recoil limit. Section 4 will include proper relativistic consideration of the Δ recoil, and will show that the corrections are visible on some plots but that they are not large. Some final comments will appear in Section 6.

2. Twisted Photons

A twisted photon is a state whose wavefront travels in a definite direction and which has arbitrary integer angular momentum along its direction of motion. Reviews may be found, for example, in refs. [13, 14]. In addition, the states studied are usually monochromatic, and at a theoretical level, one can choose between Laguerre–Gaussian or Bessel versions of these states. We here use the latter; experience has shown that results are numerically nearly the same either way, whereas analytic expressions are simpler for Bessel modes.
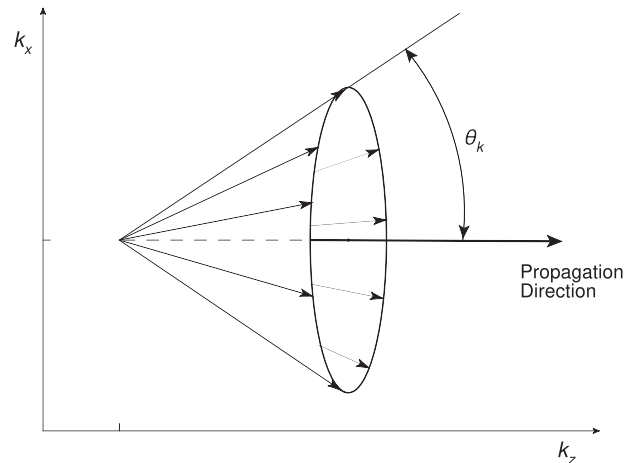

Figure 2. A twisted photon state in wavenumber space or momentum space.

Bessel photons, in addition to the twistedness and monochromaticity, are nondiffracting exact solutions to the Helmholtz equation. The states can be most simply written in wave number space, or momentum space, where they can be represented as a collection of plane wave photons, each with the same value of k_z, where z is the direction of propagation of the state, each with the same magnitude of transverse momentum $|\vec{k}_\perp| = \kappa$, and hence each with the same polar angle or pitch angle $\theta_k = \arctan(\kappa/k_z)$, but differing azimuthal angles ϕ_k. The set of wave vectors thus form a right circular cone in momentum space, **Figure 2**.

The state is [1,15,16]

$$|\kappa m_\gamma k_z \Lambda \vec{b}\rangle = A_0 \int \frac{d\phi_k}{2\pi} (-i)^{m_\gamma} e^{im_\gamma \phi_k - i\vec{k}\cdot\vec{b}} |\vec{k},\Lambda\rangle \tag{3}$$

where m_γ is the total angular momentum in the z-direction, $|\vec{k},\Lambda\rangle$ is a plane wave photon state with

$$\langle \vec{k}',\Lambda'|\vec{k},\Lambda\rangle = (2\pi)^3 \, 2\omega \delta_{\Lambda'\Lambda}\delta^3(\vec{k}'-\vec{k}) \tag{4}$$

Λ is the helicity of each component state, ω is the angular frequency of the monochromatic state, and A_0 is a normalization chosen, for example, in refs. [1, 15] as $A_0 = \sqrt{\kappa/(2\pi)}$. The state written has a vortex line passing through the point $\vec{b} = (b_x, b_y, 0)$, where we might instead give a magnitude b and azimuthal angle ϕ_b.

With this state normalization, the electromagnetic potential for a plane wave photon is

$$\langle 0|A_\mu(x)|\vec{k},\Lambda\rangle = \epsilon_\mu(\vec{k},\Lambda)e^{-ikx} \tag{5}$$

where $\epsilon_\mu(\vec{k},\Lambda)$ is a unit polarization vector for a photon of the stated momentum and helicity. The vector potential for the twisted state in coordinate space can now be worked out, and in cylindrical coordinates and for $\vec{b} = 0$ the components are

$$A_\rho = i\frac{A_0}{\sqrt{2}} e^{i(k_z z - \omega t + m_\gamma \phi)} \times \left[\cos^2\frac{\theta_k}{2}J_{m_\gamma - \Lambda}(\kappa\rho) + \sin^2\frac{\theta_k}{2}J_{m_\gamma + \Lambda}(\kappa\rho)\right]$$

**ADVANCED
SCIENCE NEWS**

www.advancedsciencenews.com

annalen
der **physik**

www.ann-phys.org

$$A_\phi = -\Lambda \frac{A_0}{\sqrt{2}} e^{i(k_z z - \omega t + m_\gamma \phi)}$$

$$\times \left[\cos^2 \frac{\theta_k}{2} J_{m_\gamma - \Lambda}(\kappa\rho) - \sin^2 \frac{\theta_k}{2} J_{m_\gamma + \Lambda}(\kappa\rho) \right]$$

$$A_z = \Lambda \frac{A_0}{\sqrt{2}} e^{i(k_z z - \omega t + m_\gamma \phi)} \sin\theta_k J_{m_\gamma}(\kappa\rho) \tag{6}$$

with $\vec{E} = i\omega\vec{A}$ and $\vec{B} = -i\Lambda\vec{E}$. The J_ν are Bessel functions. For general impact parameter, let $\vec{\rho}$ be the transverse coordinates and let $\rho \to |\vec{\rho} - \vec{b}|$.

One sometimes makes a paraxial approximation, wherein the pitch angle θ_k is small, and one keeps only the leading nontrivial terms in θ_k. We will usually not do this. Additionally, one can find exact twisted wave solutions to the Helmholtz equation where the smaller terms (for small θ_k) in A_ρ and A_ϕ above are absent,[17] with the expenses of changing the longitudinal component and of not having all the component photons in momentum space have the same helicity. We will find the uniformity in helicity useful, and so stay with the forms above.

The time averaged Poynting vector is

$$\langle S_\rho \rangle = 0$$

$$\langle S_\phi \rangle = \frac{\omega^2 A_0^2}{2} \sin\theta_k J_{m_\gamma}(\kappa\rho)$$

$$\times \left[\cos^2 \frac{\theta_k}{2} J_{m_\gamma - \Lambda}(\kappa\rho) + \sin^2 \frac{\theta_k}{2} J_{m_\gamma + \Lambda}(\kappa\rho) \right] \tag{7}$$

$$\langle S_z \rangle = \frac{\omega^2 A_0^2}{2} \left[\cos^4 \frac{\theta_k}{2} J_{m_\gamma - \Lambda}^2(\kappa\rho) - \sin^4 \frac{\theta_k}{2} J_{m_\gamma + \Lambda}^2(\kappa\rho) \right]$$

To close this section and prepare for the next, we work out the photoabsorption amplitude involving the twisted photon in the limit where the Δ is treated as very heavy and its recoil velocity is neglected. The necessary manipulations mirror the atomic physics case worked out in ref. [18]. We wish to obtain the amplitude

$$\mathcal{M} = \langle \Delta(m_f) | \mathcal{H}(0) | N(m_i); \gamma(\kappa m_\gamma k_z \Lambda \vec{b}) \rangle \tag{8}$$

where $\mathcal{H}$ is the interaction Hamiltonian density. The nucleon is at rest, and its spin projection along the z-axis is labeled as m_i. Similarly, we label the spin projection of the Δ along the same axis as m_f. The twisted photon state can be expanded in plane waves, as in Equation (3), and the plane wave photon states can be obtained by rotations of states with momenta in the z-direction,

$$|\vec{k}, \Lambda\rangle = R(\phi_k, \theta_k, 0) |k\hat{z}, \Lambda\rangle \tag{9}$$

which follows [1,15] in using the Wick phase conventions of 1962.[19]

The Hamiltonian is rotation invariant. Rotations of the nucleon states are given in terms of the Wigner functions,

$$R^\dagger(\phi_k, \theta_k, 0) |N(m_i)\rangle = e^{im_i\phi_k} \sum_{m_i'} d_{m_i, m_i'}^{1/2}(\theta_k) |N(m_i')\rangle \tag{10}$$

and rotations of the Δ can be given analogously—if the recoil velocity of the Δ is neglected. One obtains

$$\mathcal{M} = A_0(-i)^{m_f - m_i} e^{i(m_\gamma + m_i - m_f)\phi_b} J_{m_f - m_i - m_\gamma}(\kappa b)$$

$$\times \sum_{m_i'} d_{m_f, m_i' + \Lambda}^{3/2}(\theta_k) \, d_{m_i, m_i'}^{1/2}(\theta_k) \, \mathcal{M}_{m_i', \Lambda}^{(pw)} \tag{11}$$

The plane wave amplitude is defined from

$$\langle \Delta(m_f') | \mathcal{H}(0) | N(m_i'); \gamma(k\hat{z}, \Lambda) \rangle = \mathcal{M}_{m_i', \Lambda}^{(pw)} \delta_{m_f', m_i' + \Lambda} \tag{12}$$

The δ-function follows because all the spins and momenta in the plane wave amplitude are along the z-direction.

In terms of the Jones–Scadron form factors,[9,20]

$$\mathcal{M}_{1/2, 1}^{(pw)} = -\frac{3eE_\gamma}{2} \sqrt{\frac{2}{3}} \left(G_M^* + G_E^* \right)$$

$$\mathcal{M}_{-1/2, 1}^{(pw)} = -\frac{\sqrt{3} \, eE_\gamma}{2} \sqrt{\frac{2}{3}} \left(G_M^* - 3G_E^* \right) \tag{13}$$

where an isospin Clebsch–Gordan factor $\sqrt{2/3}$ for the $p \to \Delta^+$ transition is included, and

$$E_\gamma = \frac{m_\Delta^2 - m_N^2}{2m_N} = \frac{2\pi}{\lambda} \tag{14}$$

is the photon energy to excite a Δ from a nucleon at rest.[21]

3. Twisted Amplitudes for Δ Photoexcitation

When a stationary proton absorbs a photon of the correct energy to produce a $\Delta(1232)$, the Δ recoils with the momentum acquired from the photon, at a not so negligible speed of about $0.27c$. Nonethe-less, we will start by calculating the twisted photon photoexcitation amplitudes neglecting the recoil. We will find certain aspects of the no-recoil results are can be understood qualitatively, and others aspects can in simple ways be worked out analytically. In particular, that only the E2 amplitude can contribute to transitions with $\Delta m = m_f - m_i = \pm 2$ is easy to understand. Then in the next section, we will show that for crucial observables, the recoil corrections change the result in fractional terms by only about the square of half the recoil speed (in units of c).

The no-recoil result for the amplitude is like the result in an atomic transition. It is given in terms of two independent plane wave amplitudes, a pair of Wigner functions, and a Bessel function, and is shown as Equation (11) in the previous section.

We have prepared plots for a variety of m_γ, Λ, and $m_f = m_\Delta$, all for $m_i = m_p = -1/2$ and placed the results in a 4×6 grid in the Appendix. (Plots for $m_i = 1/2$ are identical if one makes the appropriate parity changes on the other quantum numbers.)

To understand the plots, we focus on two of them, shown in **Figure 3**a and b. The ordinate for both is the magnitude of the amplitude, the abscissa is the displacement of the vortex line of the twisted beam from the target proton, sweeping from the left along (say) the x-axis to the right in units of photon wavelength, λ. Both of plots are for $m_\gamma = 2$, $\Lambda = 1$, and $m_i = -1/2$. Figure 3a
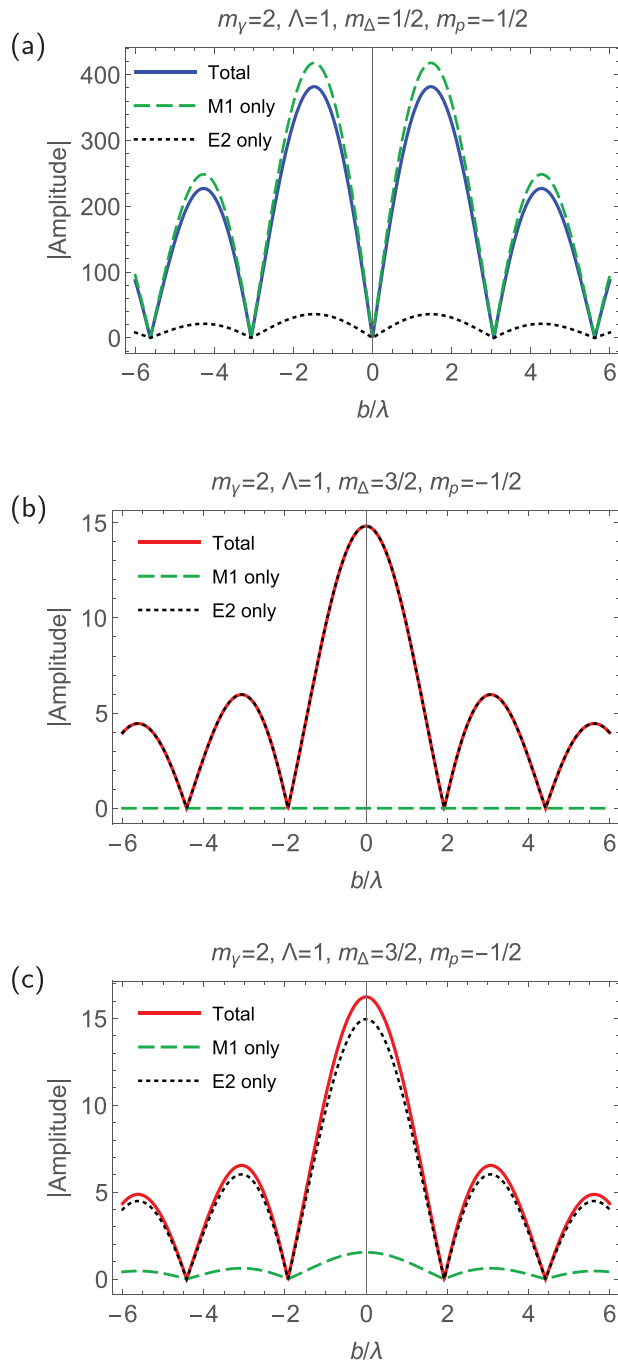
**ADVANCED
SCIENCE NEWS**

www.advancedsciencenews.com

annalen
der **physik**

www.ann-phys.org

Figure 3. Selected amplitude magnitude plots for twisted photon + proton → Δ versus displacement of the proton from the photon's vortex line, along (say) the positive and negative x-axis, in units of the photon wavelength (3.65 fm). The amplitude units are arbitrary but are the same for each figure. Each of these plots has $m_\gamma = 2$, $\Lambda = 1$, and $m_i = m_p = -1/2$. Part (a) has $m_f = m_\Delta = 1/2$ and parts (b) and (c) have $m_f = m_\Delta = 3/2$. (a) and (b) omit recoil corrections, as in Section 3. c) includes recoil corrections, as in Section 4. The E2 only curve overlays or nearly overlays the Total in parts (b) and (c). The recoil corrections are visible but small.

has $m_f = 1/2$ and Figure 3b has $m_f = 3/2$. The plots are for pitch angle $\theta_k = 0.2$.

General observations valid for all these plots, and not specific to the $N \to \Delta$, include

• *on-axis observation:* If the target sits on the vortex line, $b = 0$, the angular momentum of the photon must all go into the internal excitation of the final state, i.e., $\Delta m = m_f - m_i = m_\gamma$. If this cannot happen, the amplitude must be zero in the center, as in Figure 3a but not Figure 3b.

• *off-axis observation 1:* off-axis, the photon's total angular momentum can be shared by the internal excitation of the final state and by angular momentum of the final state overall center of mass,[22] and the amplitudes in general are not zero for $b \neq 0$.

• *off-axis observation 2:* When the target is away from the vortex line, the target sees only a piece of the swirl, which can look more unidirectional, like a plane wave. The selection rules reflect this and transitions possible with plane wave quantum numbers tend to have larger peak amplitudes than other transitions. This can be seen by comparing the vertical scales in Figure 3a,b.

Specific to the $N \to \Delta$ transition are the separate contributions of the M1 and E2 amplitudes, which are shown in the plots. Most interesting is Figure 3b, where the M1 does not contribute at all. A measurement with the final Δ constrained to be in the projection $m_f = 3/2$ state would give a direct measurement of the E2 amplitude.

The plots are for $G_E^*/G_M^* = 3\%$, and Figure 3a shows the a more usual case where the M1 gives the major share of the amplitude.

Further regarding the absence of M1 contribution to the $\Delta m = m_f - m_i = 2$ transition, there are only two terms in the sum for the amplitude, Equation (11), so it is easy to insert explicit Wigner functions and plane wave amplitudes in terms of M1 and E2, Equation (13), and demonstrate analytically that the M1 contribution cancels. This is true for any $\Delta m = 2$ transition, and one can see this in the plots in the Appendix, where every plot in the right hand column has $\Delta m = 2$ and no M1 contribution.

4. Recoil Momentum Corrections

The Δ recoils when it is produced by the proton absorbing the photon. The rotations of the moving state are not given so simply as for a state at rest. It will turn out that the corrections are not numerically large, but we want to consider them.

We find it here helpful to consider the wave function of the initial nucleon state. The theory is simplest when the target is localized both in coordinate space and in momentum. One of these makes it possible to write results using helicity amplitudes defined for plane waves, the other will show the expected result that the Delta comes only from where the target proton was located. We of course realize that there is a playoff between uncertainty in target localization and uncertainty of target momentum. We shall treat the uncertainties in both position and momentum as small judged by to scales over which other quantities in the calculation vary.[23,24] This is standard in atomic physics, and appears feasible here also. For comparison, even situations in particle or nuclear physics that ultimately involve only plane waves have the manipulations involved in scattering theory justified by using wave packets for the states—see, for example, refs. [23, 24]—and then taking limits.

ADVANCED
SCIENCE NEWS

www.advancedsciencenews.com

annalen
der physik

www.ann-phys.org

The amplitude is

$$\mathcal{M} = \int (d^3p) \widetilde{\phi}_i(\vec{p}_i) \times \langle \Delta(p_f, m_f') | H | N(\vec{p}_i, m_i), \gamma(\kappa m_\gamma k_z \Lambda \vec{b}) \rangle \quad (15)$$

where H is the interaction Hamiltonian and (d^3p) is $d^3p/(2\pi)^3$. Inserting the expansion for the twisted photon gives

$$\mathcal{M} = A_0 \int \frac{d\phi_k}{2\pi} (-i)^{m_\gamma} e^{im_\gamma \phi_k - i\vec{k}\cdot\vec{b}} \widetilde{\phi}_i(\vec{p}_i)$$
$$\times \langle \Delta(p_f, m_f') | \mathcal{H}(0) | N(\vec{p}_i, m_i), \gamma(\vec{k}, \Lambda) \rangle \quad (16)$$

where $\vec{p}_f = \vec{p}_i + \vec{k}$. Further,

$$\mathcal{M} = A_0 \int \frac{d\phi_k}{2\pi} (-i)^{m_\gamma} e^{i(m_\gamma + m_i)\phi_k - i\vec{k}\cdot\vec{b}} \widetilde{\phi}_i(\vec{p}_f - \vec{k})$$
$$\times \mathcal{M}^{(\mathrm{pw})}_{m_i'\Lambda} d^{1/2}_{m_i m_i'}(\theta_k) \quad (17)$$

with $m_f' = m_i' + \Lambda$. This supposes that the wave function peaks sharply enough so that we can evaluate the plane wave amplitude at $\vec{p}_i = 0$, and do rotations on the nucleon as if it were at rest. There is only one Wigner function, because we have not yet projected the Δ onto states with spin quantized along the z-axis.

This is the amplitude for producing $|\Delta(\vec{p}_f, m_f')\rangle$. The whole of the Δ final state is

$$|f\rangle = \sum_{m_f'} \int \frac{(d^3p_f)}{2E_f} |\Delta(\vec{p}_f, m_f')\rangle (-i)^{m_\gamma} e^{i(m_\gamma + m_i)\phi_k - i\vec{k}\cdot\vec{b}}$$
$$\times \widetilde{\phi}_i(\vec{p}_f - \vec{k}) \mathcal{M}^{(\mathrm{pw})}_{m_i'\Lambda} d^{1/2}_{m_i m_i'}(\theta_k) \quad (18)$$

We get the coordinate wave function of this state using the Δ field operator and

$$\langle 0 | \Psi_\mu(x) | \Delta(\vec{p}_f, m_f') \rangle = u_\mu(\vec{p}_f, m_f') e^{-ip_f \cdot x} \quad (19)$$

leaving

$$\langle 0 | \Psi_\mu(x) | f \rangle = \sum_{m_f'} \int \frac{d\phi_k}{2\pi} \frac{u_\mu(\vec{p}_f, m_f')}{2E_f} (-i)^{m_\gamma}$$
$$\times e^{i(m_\gamma + m_i)\phi_k - i\vec{k}\cdot\vec{b}} \phi_i(\vec{x}) \mathcal{M}^{(\mathrm{pw})}_{m_i'\Lambda} d^{1/2}_{m_i m_i'}(\theta_k) \quad (20)$$

at time zero. The peaking of the wave function gives $\vec{p}_f = \vec{k}$, and the angles for the outgoing Δ that we might call $\theta_\Delta, \phi_\Delta$ are the same a θ_k, ϕ_k.

The Rarita–Schwinger spin-3/2 spinors are given in terms of spin-1 polarization vectors and spin-1/2 Dirac spinors as

$$u_\mu(\vec{p}, m) = \sum_{\lambda,\mu} \begin{pmatrix} 3/2 & 1 & 1/2 \\ m & \lambda & \mu \end{pmatrix} \epsilon_\mu(\hat{p}, \lambda) u(\vec{p}, \mu) \quad (21)$$

Given the structure of the Dirac spinor, one can define a two-spinor with a vector index

$$\chi_\mu(\hat{p}, m) = \sum_{\lambda,\mu} \begin{pmatrix} 3/2 & 1 & 1/2 \\ m & \lambda & \mu \end{pmatrix} \epsilon_\mu(\hat{p}, \lambda) \chi(\hat{p}, \mu) \quad (22)$$

where χ is a two-component spin-1/2 helicity state. Thence,

$$u_\mu(\vec{p}, m) = \frac{1}{\sqrt{E_\Delta + M_\Delta}} \begin{pmatrix} (E_\Delta + M_\Delta) \chi_\mu(\hat{p}, m) \\ \vec{\sigma} \cdot \vec{p} \, \chi_\mu(\hat{p}, m) \end{pmatrix} \quad (23)$$

where the $\vec{\sigma}$ are the 2×2 Pauli matrices.

Under rotations, ϵ_μ and χ transform simply using the Wigner functions d^1 and $d^{1/2}$, respectively, and with Wigner function theorems [25,26] one can show that

$$\chi_\mu(\hat{p}, m) = R\chi_\mu(\hat{z}, m) = \sum_{m'} e^{-i\phi_k} d^{3/2}_{mm'}(\theta_k) \chi_\mu(\hat{z}, m') \quad (24)$$

with $R = R(\phi_k, \theta_k, 0)$. This means that the upper components of the Rarita–Schwinger spin or will transform under rotations with the same application of the Wigner functions as for a state at rest. This means that one can do the same manipulations as for the no-recoil case, and obtain results that look like the nonrelativistic case, Equation (11). This in turn means that although the final Δ is not a momentum eigenstate, one can express the upper components, and hence the numerical bulk of the state, in terms of momentum eigenstate u_μ spinors with momenta in the z-direction.

However, for the lower components there is additional angular dependence in the $\vec{\sigma} \cdot \vec{p}$ term. In particular,

$$\vec{\sigma} \cdot \hat{k} = \sigma_+ \sin \theta_k e^{-i\phi_k} + \sigma_- \sin \theta_k e^{+i\phi_k} + \sigma_z \cos \theta_k \quad (25)$$

where $\sigma_\pm = \sigma_x \pm i\sigma_y$. One can still do the azimuthal integral, but the extra ϕ_k dependence will bring in Bessel functions with different indices from the main term.

Doing the integral, and projecting onto the z-direction spinor $\bar{u}^\mu(p\hat{z}, m_f)$ leads to a main term that looks the same as the no-recoil result Equation (11) (albeit with a factor of the target wave function) plus a correction term which we will have the temerity to write out,

$$\delta\mathcal{M} = A_0 \, i^{(m_i - m_f)} e^{i(m_i + m_\gamma - m_f)\phi_b} \frac{M_\Delta - E_\Delta}{2M_\Delta} \sum_{m_i'}$$

$$\left\{ \begin{pmatrix} 3/2 & 1 & 1/2 \\ m_f & m_f - 1/2 & 1/2 \end{pmatrix} \begin{pmatrix} 3/2 & 1 & 1/2 \\ m_f - 1 & m_f - 1/2 & -1/2 \end{pmatrix} \right.$$

$$\times \sin \theta_k \, d^{3/2}_{m_f - 1, m_i' + \Lambda}(\theta_k)$$

$$+ \begin{pmatrix} 3/2 & 1 & 1/2 \\ m_f & m_f + 1/2 & -1/2 \end{pmatrix} \begin{pmatrix} 3/2 & 1 & 1/2 \\ m_f + 1 & m_f + 1/2 & 1/2 \end{pmatrix}$$

$$\times \sin \theta_k \, d^{3/2}_{m_f + 1, m_i' + \Lambda}(\theta_k)$$

$$\left. + (\cos \theta_k - 1) \, d^{3/2}_{m_f, m_i' + \Lambda}(\theta_k) \right\}$$

$$\times \phi_i(x) \mathcal{M}^{(\mathrm{pw})}_{m_i', \Lambda} J_{m_f - m_\gamma - m_i}(\kappa b) \, d^{1/2}_{m_i, m_i'}(\theta_k) \quad (26)$$
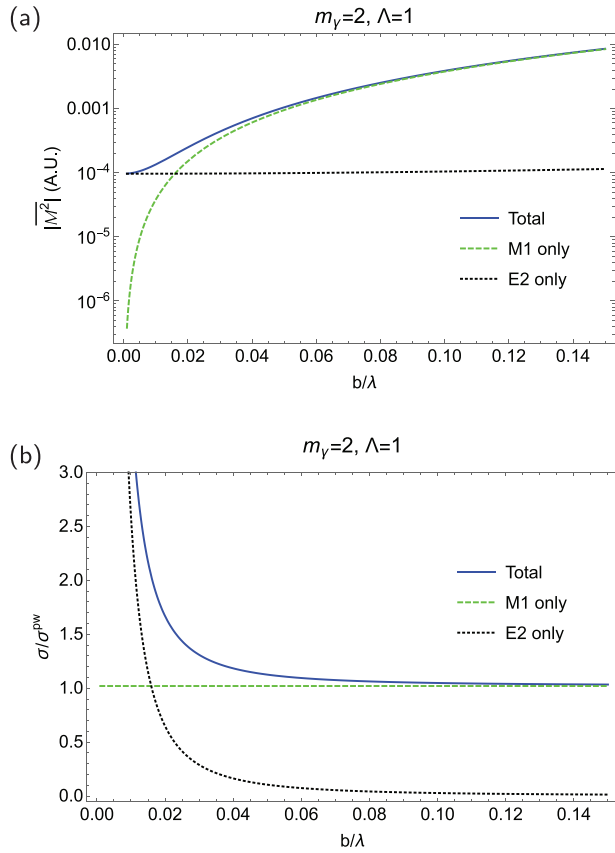
(a)

(b)

Figure 4. a) Matrix element squared, $|\overline{\mathcal{M}}|^2$, with summation/averaging performed over baryon helicities. We choose the photon helicity $\Lambda = 1$ and total angular momentum projection $m_\gamma = 2$. The blue solid line includes both $M1$ and $E2$ transitions, while the green dashed (black dotted) lines show individual contributions from $M1$ ($E2$). b) Same as a) divided by the photon energy flux density obtainable from Equation (6) and normalized to the plane-wave limit $m_\gamma = 1$, $\theta_k \to 0$.

The nominal size of the correction term is

$$\frac{E_\Delta - M_\Delta}{2M_\Delta} = \frac{k^2}{2M_\Delta(E_\Delta + M_\Delta)} \approx 1.9\% \tag{27}$$

as already noted in the introduction.

Implementing the corrections, the amplitude with projection onto the final Δ state with $m_f = 3/2$ is shown in Figure 3c. The amplitude in Figure 3 is given in arbitrary units; in particular the factor A_0, which is determined by the intensity of the incoming wavefront, is omitted and the target wave function is taken at some argument where the result is non-zero, but otherwise also omitted. The extra terms have some effect, as seen, but very small. The corresponding corrections for other quantum number situations are visually even smaller.

5. Rates, Cross Sections, and Novel Spin Effects

Squaring the twisted amplitudes Equation (11), summing over final helicities of Δ and averaging over initial helicities of a nucleon, we obtain a quantity $|\overline{\mathcal{M}}|^2$ that defines a transition rate for photoexcitation. The result is shown in **Figure 4**a as a function
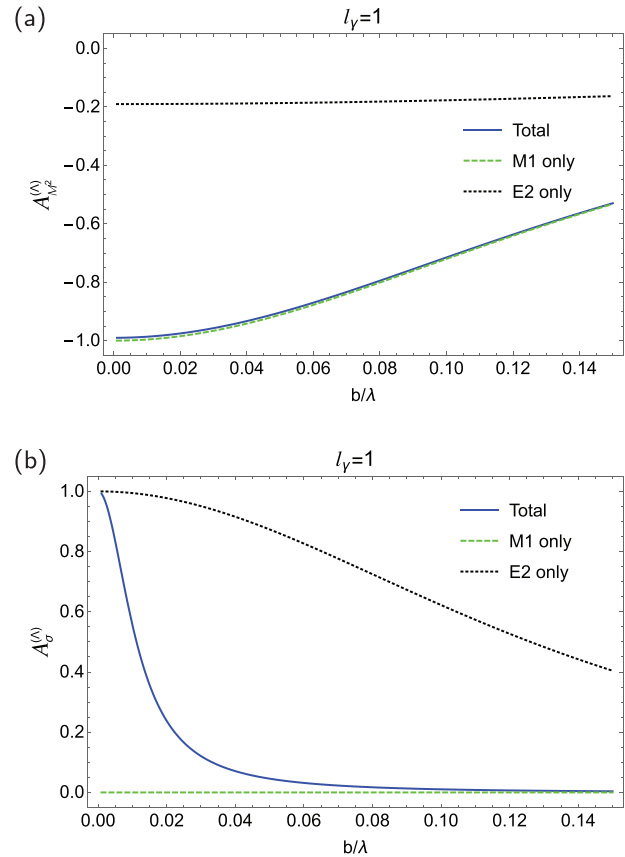
(a)

(b)

Figure 5. Beam spin asymmetry for the transition rate (a) and flux-normalized cross section (b) as defined in Equations (28) and (29). We took $l_\gamma = 1$; notation for the curves is as in Figure 4.

of proton's transverse position b with respect to the twisted photon's axis.

It can be seen that the contribution of the electric quadrupole amplitude $E2$ is almost independent of b, whereas the magnetic dipole $M1$ contribution is suppressed in the vicinity of the photon vortex center as $b \to 0$. Since this rate is obtained with a position-dependent photon flux, it is instructive to divide the rate by the flux, defining a position-dependent cross section $\sigma(b)$ of photoexcitation shown in Figure 4b.

The outcome shows a remarkable feature of the twisted photoexcitation: For $E2$ transitions the rate remains nonzero as $b \to 0$, while the flux turns to zero. It effectively leads to an infinite cross section seen in Figure 4b at the vortex center. On the other hand, $M1$ absorption rate is proportional to the flux, same as for the cross-section of plane-wave photoabsorption.

Next, we compare absorption rates and cross sections for different values of photon helicity Λ, while keeping fixed the quantity $l_\gamma = m_\gamma - \Lambda$ that corresponds to photon's orbital angular momentum (in a paraxial limit). Namely, we form the following asymmetries:

$$A_{\mathcal{M}^2}^{(\Lambda)} = \frac{|\overline{\mathcal{M}}|^2_{\Lambda=1} - |\overline{\mathcal{M}}|^2_{\Lambda=-1}}{|\overline{\mathcal{M}}|^2_{\Lambda=1} + |\overline{\mathcal{M}}|^2_{\Lambda=-1}} \tag{28}$$

**ADVANCED
SCIENCE NEWS**

www.advancedsciencenews.com

annalen
der **physik**

www.ann-phys.org

$m_\gamma = -2, \Lambda = -1, m_i = -1/2, m_f = -3/2$ to $+3/2$

$m_\gamma = -1, \Lambda = -1, m_i = -1/2, m_f = -3/2$ to $+3/2$

$m_\gamma = 0, \Lambda = -1, m_i = -1/2, m_f = -3/2$ to $+3/2$

$m_\gamma = 0, \Lambda = 1, m_i = -1/2, m_f = -3/2$ to $+3/2$

$m_\gamma = 1, \Lambda = 1, m_i = -1/2, m_f = -3/2$ to $+3/2$

$m_\gamma = 2, \Lambda = 1, m_i = -1/2, m_f = -3/2$ to $+3/2$

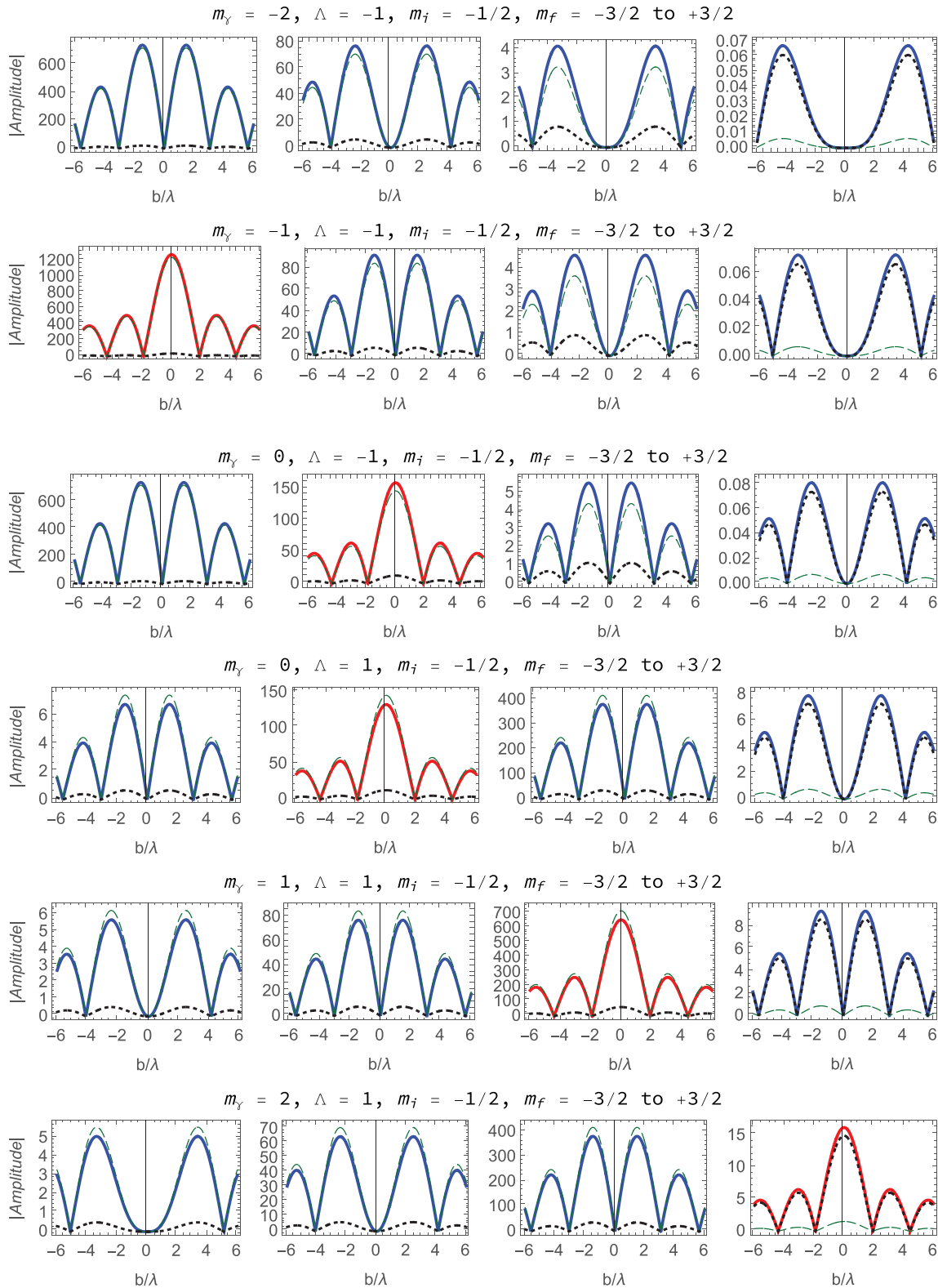**Figure A.1.** Plots of amplitudes for $\gamma + p \to \Delta$ with twisted photons. The protons all have spin projection $m_i = -1/2$. The m_γ and Λ for each row are labeled, and the spin projections of the final Δ run from $-3/2$ to $+3/2$. left to right. The units of the amplitude are arbitrary, but are the same for each plot. The pitch angle for each plot is $\theta_k = 0.2$. The red (for $m_\gamma = \Delta m$) or blue (otherwise) solid curves are the total; the green dashed curves are G_M^* alone and the black dotted curves are G_E^* alone.

i.e., the beam spin asymmetry of transition rate and

$$A_\sigma^{(\Lambda)} = \frac{\sigma_{\Lambda=1} - \sigma_{\Lambda=-1}}{\sigma_{\Lambda=1} + \sigma_{\Lambda=-1}} \tag{29}$$

or the beam spin asymmetry of cross sections. Both these asymmetries would be identically zero for plane-wave photons if spatial parity is conserved. They may be nonzero for the twisted photons because they arise due to the differences between twisted photoabsorption with aligned vs. anti-aligned spin (Λ) with respect to the orbital angular momentum (l_γ). A similar effect for atomic transitions was predicted theoretically in, ref.[27] with $E2$ transitions shown to be responsible for cross-sectional asymmetries.

The results shown in **Figure 5** demonstrate that the spin asymmetry of transition rate is dominated by $M1$ transition similarly to spin dependence of the photon flux, but the asymmetry of cross section is dominated by $E2$ contribution near the photon vortex center.

The differences in contributions of $E2$ and $M1$ transitions in the twisted photoabsorption can be better understood from comparing analytic expressions if we perform a Taylor expansion of the cross section near the vortex center in a paraxial limit (c.f. Equations (21)–(24) of ref.[12]):

$$\sigma_{(m_\gamma=2,\Lambda=1)} \propto 3G_E^{*2} + G_M^{*2} + \frac{3G_E^{*2}}{(b\pi/\lambda)^2} \tag{30}$$

Comparing the expression above with the plane-wave cross section

$$\sigma^{pw} \propto 3G_E^{*2} + G_M^{*2} \tag{31}$$

it becomes apparent that the twisted cross section has a $1/b^2$ singularity near the vortex center exclusively due to the $E2$ amplitude G_E^*.

6. Summary

We have considered photoproduction of the $\Delta(1232)$ baryon by twisted photons. The angular momentum selection rules for the transitions to definite final states are different from what is possible with plane waves, and leads to additional opportunities. In particular, there are transitions to which the main $M1$ component does not contribute at all in the no-recoil or nonrelativistic limit, and even with corrections implemented, contributes only very slightly. A measurement of these transitions can isolate and measure the smaller $E2$ amplitude, which is a measure of the more complete structure of the baryon states.

Twisted photon experiments like these are clearly for the future. One needs good control over the final energy and momentum direction of twisted photons so that the pitch angle θ_k remains much larger than beam's angular spread in generation, e.g., by backscattering visible photons from an energetic electron beam. The CEBAF 12 GeV electron beam currently delivered to Hall D (for example) has an energy spread of only 2.2 MeV [28] and angular spread $0.1/\gamma$ in radians, where γ is the Lorentz factor of he electron beam.[29] Laser produced visible photons are also precise in energy and direction, so maintaining spreads of this com-

pactness should be feasible and certainly adequate. More problematic is learning how to produce the energetic twisted photons with large pitch angles and with good control over the location of the photon's vortex axis relative to the target. However, there are good opportunities, and since gamma factories are under consideration, twisted photon beams should also be considered.

Appendix: Larger Collection of Plots

Figure A.1 presents a set of plots for twisted photon + proton → $\Delta(1232)$, with varying choices for the twisted photon total angular momentum m_γ, photon helicity Λ, and final Δ spin projection m_f. The vertical axis shows the amplitude magnitudes, and the horizontal axis shows the impact parameter or the offset between the target location and the photon vortex axis.

All plots have the proton polarized with $m_i = -1/2$. Plots with $m_i = +1/2$ are identical if one uses parity to change the other quantum numbers appropriately. Each row has m_γ and Λ, the helicity of the incoming photons in a Fourier decomposition, labeled. In each row the spin projection of the final Δ goes from $-3/2$ on the left to $+3/2$ on the right.

These plots include the recoil corrections. One notices that all plots in the right-hand column show only small contribution from the elsewhere dominant $M1$ amplitude.

Conflict of Interest

The authors declare no conflict of interest.

Data Availability Statement

Data sharing is not applicable to this article as no new data were created or analyzed in this study.

[1] U. Jentschura, V. Serbo, *Eur. Phys. J. C* **2011**, *71*, 1571.
[2] V. Petrillo, G. Dattoli, I. Drebot, F. Nguyen, *Phys. Rev. Lett.* **2016**, *117*, 123903.
[3] D. Budker, J. R. Crespo López-Urrutia, A. Derevianko, V. V. Flambaum, M. W. Krasny, A. Petrenko, S. Pustelny, A. Surzhykov, V. A. Yerokhin, M. Zolotorev, *Ann. Phys. (Berlin, Ger.)* **2020**, *532*, 2000204.
[4] P. Liu, J. Yan, A. Afanasev, S. V. Benson, H. Hao, S. F. Mikhailov, V. G. Popov, Y. K. Wu, arXiv:2007.15723, **2020**.

[5] M. Drechsler, S. Wolf, C. T. Schmiegelow, F. Schmidt-Kaler, arXiv:2104.07095, **2021**.

[6] C. T. Schmiegelow, J. Schulz, H. Kaufmann, T. Ruster, U. G. Poschinger, F. Schmidt-Kaler, *Nat. Commun.* **2016**, *7*, 12998.

[7] A. Afanasev, C. E. Carlson, C. T. Schmiegelow, J. Schulz, F. Schmidt-Kaler, M. Solyanik, *New J. Phys.* **2018**, *20*, 023032.

[8] M. Solyanik-Gorgone, A. Afanasev, C. E. Carlson, C. T. Schmiegelow, F. Schmidt-Kaler, *J. Opt. Soc. Am. B* **2019**, *36*, 565.

[9] V. Pascalutsa, M. Vanderhaeghen, S. N. Yang, *Phys. Rep.* **2007**, *437*, 125.

[10] P. A. Zyla, et al. (Particle Data Group), *Prog. Theor. Exp. Phys.* **2020**, *2020*, 083C01.

[11] P. Rynkun, P. Jönsson, G. Gaigalas, C. F. Fischer, *At. Data Nucl. Data Tables* **2012**, *98*, 481, (The specific transition is $^2P_{1/2} \to {}^2D_{3/2}$ (142 nm) on p. 501 of this article. Both states have 3 electrons in a $2s2p^2$ configuration. The atom in question is Ne VI, which has 5 electrons, the same as neutral Boron.).

[12] A. Afanasev, C. E. Carlson, M. Solyanik, *Phys. Rev. A* **2018**, *97*, 023422.

[13] A. M. Yao, M. J. Padgett, *Adv. Opt. Photonics* **2011**, *3*, 161.

[14] K. Y. Bliokh, F. Nori, *Phys. Rept.* **2015**, *592*, 1.

[15] U. Jentschura, V. Serbo, *Phys. Rev. Lett.* **2011**, *106*, 013001.

[16] A. Afanasev, C. E. Carlson, A. Mukherjee, *Phys. Rev. A* **2013**, *88*, 033841.

[17] G. F. Quinteiro, C. T. Schmiegelow, D. E. Reiter, T. Kuhn, *Phys. Rev. A* **2019**, *99*, 023845.

[18] H. M. Scholz-Marggraf, S. Fritzsche, V. G. Serbo, A. Afanasev, A. Surzhykov, *Phys. Rev. A* **2014**, *90*, 013425.

[19] G. C. Wick, *Ann. Phys. (Amsterdam, Neth.)* **1962**, *18*, 65.

[20] H. F. Jones, M. D. Scadron, *Ann. Phys. (Amsterdam, Neth.)* **1973**, *81*, 1.

[21] Equation (13) was obtained using ref. [9] and agrees with ref. [20] if one identifies $\mathcal{H}(0)$ here with $-ie\Gamma$ there and also inserts the isospin factor.

[22] A. Afanasev, C. E. Carlson, A. Mukherjee, *J. Opt. Soc. Am. B Opt. Phys.* **2014**, *31*, 2721.

[23] J. R. Taylor, *Scattering Theory: The Quantum Theory of Nonrelativistic Collisions*, Dover, Mineola, NY, USA **2006**, Chs. 2 and 3 (originally Wiley, New York (1972) and also Krieger, Malabar, Florida (1983)).

[24] M. E. Peskin, D. V. Schroeder, *An Introduction to Quantum Field Theory*, Addison-Wesley, Reading, PA, USA **1995**, Sec. 4.5.

[25] M. E. Rose, *Elementary Theory of Angular Momentum*, John Wiley and Sons, New York **1957**.

[26] A. R. Edmonds, *Angular Momentum in Quantum Mechanics*, Princeton University Press, Princeton, NJ, USA **1957**.

[27] A. Afanasev, C. E. Carlson, M. Solyanik, *J. Opt.* **2017**, *19*, 105401.

[28] S. Adhikari, et al., *Nucl. Instrum. Meth. A* **2021**, *987*, 164807.

[29] G. A. Krafft, J. C. Denard, R. W. Dickson, R. Kazimi, V. A. Lebedev, M. G. Tiefenback, *eConf* **2000**, *C00082*, TH205.